DATA REPORT

X-ray powder diffraction data and characterization of Mirabegron

Jose H. Quintana Mendoza,[1,2,3,a)] J. A. Henao,[1] Andrea P. Aparicio,[1] and Arnold R. Romero Bohorquez[1,2]
[1]*Grupo de Investigación en Química Estructural (GIQUE), Escuela de Química, Facultad de Ciencias, Universidad Industrial de Santander, A.A. 678, Carrera 27, Calle 9 Ciudadela Universitaria. Bucaramanga, Colombia*
[2]*Grupo de Investigación en Compuestos Orgánicos de Interés Medicinal (CODEIM), Parque Tecnológico Guatiguará, Universidad Industrial de Santander, A.A. 678, Piedecuesta, Colombia*
[3]*Grupo de Investigación en Biocalorimetría, Departamento de Química, Universidad de Pamplona, Km 1 vía Bucaramanga, Pamplona, Colombia*

(Received 30 May 2017; accepted 12 October 2017)

Mirabegron, ($C_{21}H_{24}N_4O_2S$), is a β_3-adrenoceptor agonist approved in Japan, the USA, Canada and Europe, for the treatment of overactive bladder symptoms. There are no entries for this important active pharmaceutical ingredient in the Cambridge Structural Database or the Powder Diffraction File-4/Organics database. In this contribution, the powder diffraction pattern of Mirabegron, an unreported phase, are presented with a study by spectroscopy methods (Fourier-transform infrared spectroscopy [FT-IR] and RAMAN) and thermal analysis (thermogravimetric analysis [TGA]-differential scanning calorimetry [DSC]). © *2017 International Centre for Diffraction Data*.
[doi:10.1017/S0885715617001129]

Key words: Mirabegron, characterization, X-ray powder diffraction

I. INTRODUCTION

Mirabegron (Figure 1), an active pharmaceutical ingredient (API) approved in Japan, the USA, Canada and Europe, used for the symptomatic treatment of urgency, increased micturition frequency and/or urgency incontinence as may occur in adult patients with overactive bladder (OAB) syndrome. Mirabegron is a potent and selective β_3-adrenoceptor agonist (Nitti *et al.*, 2013).

There are no entries for this important API in the Cambridge Structural Database (CSD) (Groom *et al.*, 2016) or the Powder Diffraction File (PDF)-4/Organics database. A study by spectroscopy methods (Fourier-transform-infrared spectroscopy (FT-IR), RAMAN), thermal analysis [thermogravimetric analysis (TGA)-differential scanning calorimetry (DSC)] and X-ray powder diffraction of this material, crystallized from a commercial product, was carried out as part of our interest in the structural characterization of pharmaceuticals compounds.

II. EXPERIMENTAL

A. Extraction and crystallization

Commercial Mirabegron was dissolved in a mixture of isopropanol: water. After filtering, the extract was crystallized by the solvothermal method in an autoclave under heating at 60 °C for 4 h. The density of the crystals was determined by the floatation method using potassium iodide solution.

B. IR and RAMAN spectroscopy

The FT-IR spectrum was measured in a IS50 FT-IR Nicolet Thermo Scientific spectrophotometer over the range 4000–400 cm^{-1} with 32 scans per sample in KBr pellets. RAMAN spectrum was recorded in a LabRam HR Evolution using a laser at 532 nm with 100% attenuation to 3 s. in a range of 1700–800 cm^{-1} owing to fluorescence sample.

C. Thermal analysis, TGA-DSC

Thermal analysis TGA-DSC were performed in a Thermal Analyzer differential thermal analysis/DSC Instrument Serie Discovery, both experiments under a nitrogen atmosphere with mass flow 50.0 ml min^{-1}, equilibrate at 25 °C, ramp at 10 °C min^{-1} to 500 °C for TGA and 550 °C for DSC analysis.

C. X-ray powder diffraction data collection

Powder diffraction patterns were recorded at room temperature on a BRUKER D8 ADVANCE diffractometer

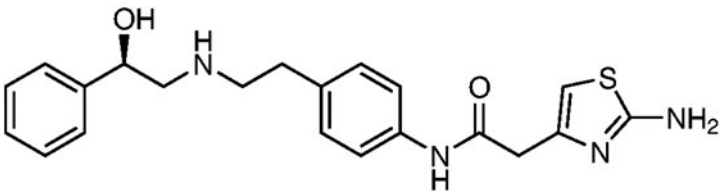

Figure 1. Chemical structure of mirabegron.

a)Author to whom correspondence should be addressed. Electronic mail: jhquintanam@gmail.com

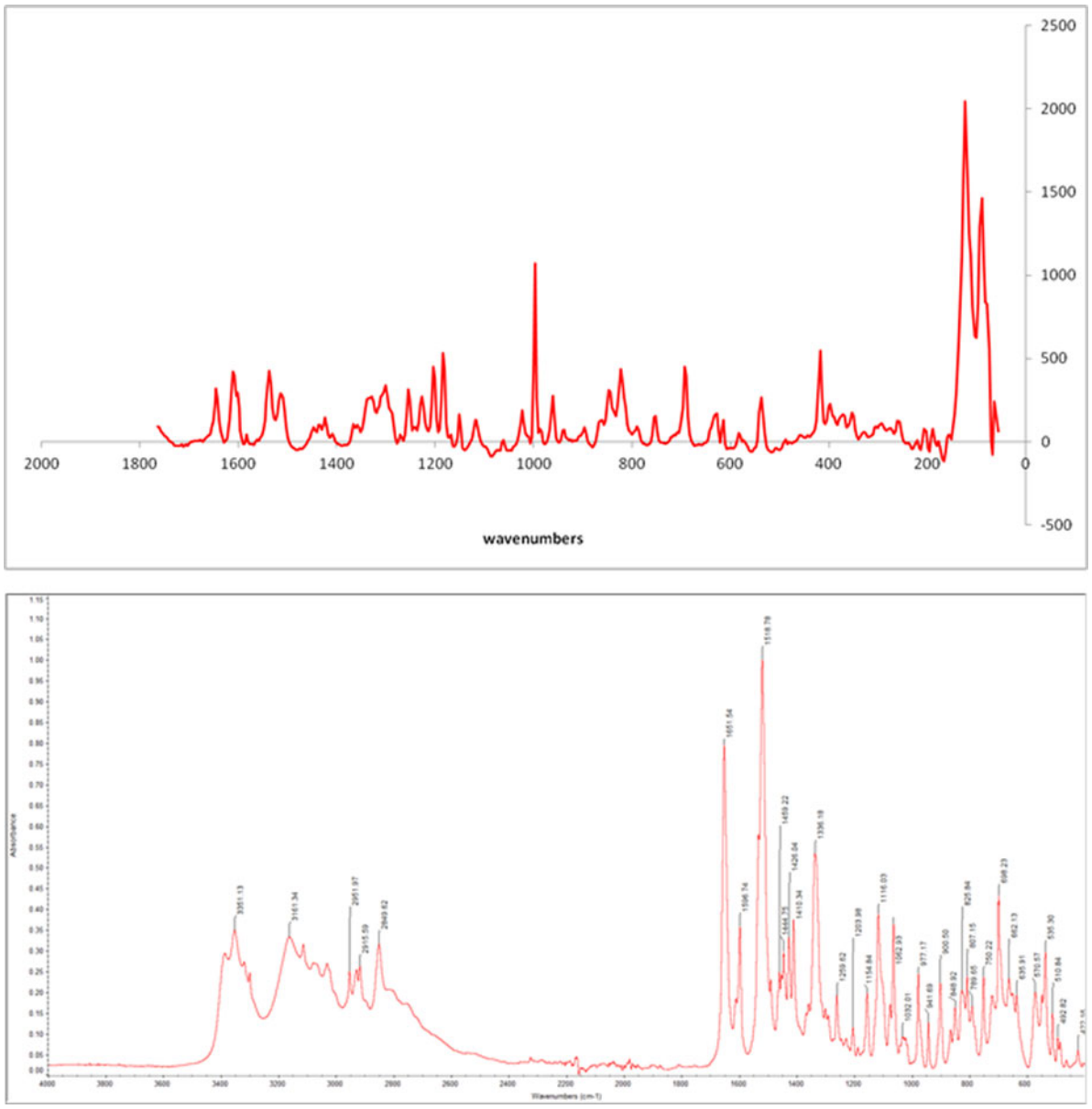

Figure 2. (Colour online) RAMAN spectrum (top) and IR spectrum (bottom) of mirabegron.

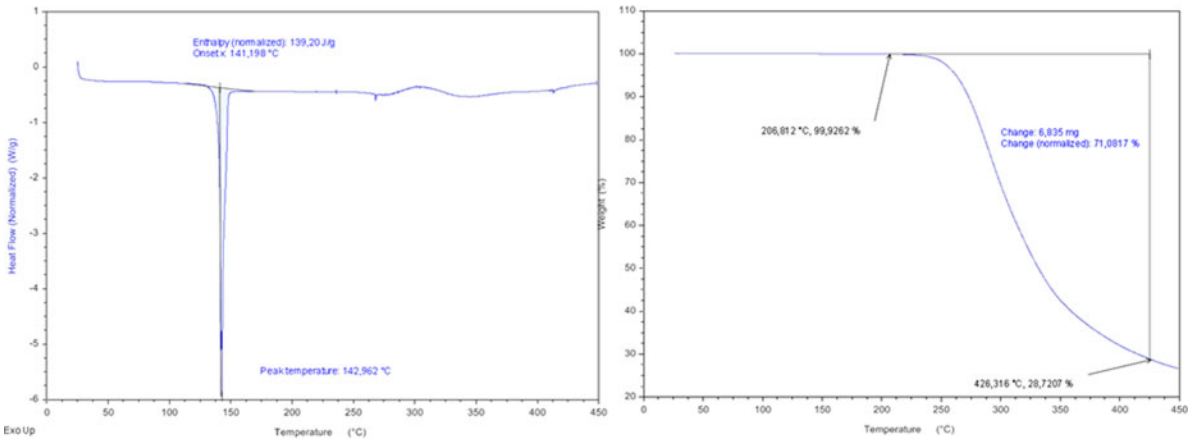

Figure 3. (Colour online) DSC (right) curve and TGA curve (left) of mirabegron.

https://doi.org/10.1017/S0885715617001129 Published online by Cambridge University Press

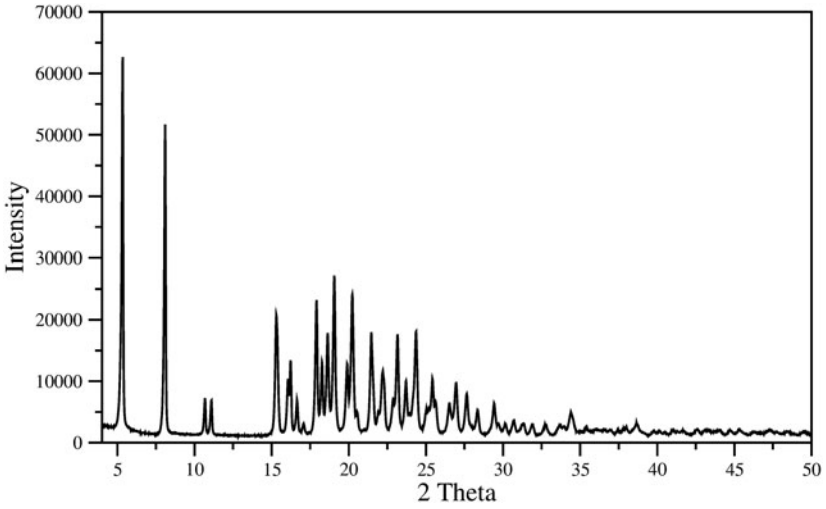

Figure 4. Powder diffraction pattern of mirabegron.

using Cu$K\alpha$ radiation, operating at 40 kV and 40 mA, in steps of 0.0156° (2θ), from 4° to 50° at 1 s per step. The diffractometer was equipped with the primary and secondary Soller slits of 2.5°, divergence slit of 0.6 mm, Nickel filter of 0.02 mm, and a LynxEye detector. The fitting and subtraction of background, using the Sonneveld and Visser (1975) method, smoothing by sliding polynomials (Savitzky and Golay, 1964) and $K\alpha_2$-stripping (Rachinger, 1948) were performed using PowderX program (Dong, 1999); the second derivative method was used to determine the peak observed positions.

III. RESULTS AND DISCUSSION

Raman spectrum (Figure 2) shows a strong band at 997 cm^{-1}, corresponding to the vibration C–S. The vibration

TABLE I. X-ray powder diffraction data of mirabegron.

$2\theta_{obs}$ (°)	d_{obs} (Å)	$(I/I_0)_{obs}$	h	K	L	$2\theta_{calc}$ (°)	d_{calc} (Å)	$\Delta 2\theta$ (°)
5.341	16.5328	1000	0	0	1	5.333	16.5573	−0.008
8.090	10.9201	825	0	1	1	8.093	10.9160	0.003
10.668	8.2862	90	0	0	2	10.678	8.2787	0.010
11.082	7.9776	87	0	1	2	11.096	7.9674	0.014
15.299	5.7868	327	0	2	1	15.280	5.7938	−0.019
16.049	5.5180	144	0	0	3	16.046	5.5191	−0.003
16.214	5.4623	192	0	2	2	16.227	5.4580	0.013
16.634	5.3253	87	1	0	0	16.644	5.3221	0.010
17.056	5.1945	26	1	0	1	17.071	5.1900	0.015
17.893	4.9533	353	−1	0	1	17.898	4.9519	0.005
18.251	4.8569	189	1	1	0	18.261	4.8543	0.010
18.619	4.7618	267	0	−2	1	18.623	4.7609	0.004
19.046	4.6560	423	1	1	2	19.062	4.6520	0.016
19.883	4.4618	185	1	−1	1	19.882	4.4620	−0.001
20.214	4.3895	378	0	−1	3	20.214	4.3894	0.000
20.524	4.3239	53	−1	0	2	20.536	4.3213	0.012
20.983	4.2303	4	−1	1	2	20.988	4.2293	0.005
21.452	4.1389	271	0	0	4	21.450	4.1393	−0.002
21.572	4.1161	156	1	1	3	21.575	4.1157	0.003
21.915	4.0525	55	1	2	1	21.913	4.0529	−0.002
22.181	4.0045	166	0	−2	2	22.157	4.0088	−0.024
22.278	3.9873	143	1	−1	2	22.283	3.9864	0.005
22.867	3.8859	91	1	2	0	22.867	3.8859	0.000
23.144	3.8400	269	0	3	1	23.148	3.8393	0.004
23.694	3.7521	140	−1	2	0	23.689	3.7529	−0.005
23.926	3.7162	49	−1	1	3	23.923	3.7167	−0.003
24.149	3.6824	113	−1	0	3	24.128	3.6856	−0.021
24.345	3.6532	280	−1	2	2	24.343	3.6535	−0.002
25.033	3.5543	65	1	1	4	25.034	3.5542	0.001
25.201	3.5310	68	1	−2	1	25.166	3.5359	−0.035
25.413	3.5020	149	0	1	5	25.424	3.5005	0.011
25.618	3.4745	85	1	−1	3	25.631	3.4727	0.013
26.314	3.3841	23	0	−2	3	26.362	3.3781	0.048

Continued

https://doi.org/10.1017/S0885715617001129 Published online by Cambridge University Press

TABLE I. Continued

$2\theta_{obs}$ (°)	d_{obs} (Å)	$(I/I_0)_{obs}$	h	K	L	$2\theta_{calc}$ (°)	d_{calc} (Å)	$\Delta 2\theta$ (°)
26.508	3.3598	84	1	2	4	26.513	3.3592	0.005
26.600	3.3484	53	0	−3	1	26.622	3.3457	0.022
26.940	3.3069	142	−1	−1	3	26.948	3.3060	0.008
27.631	3.2258	112	1	3	2	27.631	3.2257	0.000
27.856	3.2002	29	1	3	1	27.869	3.1987	0.013
28.336	3.1471	69	−1	0	4	28.338	3.1469	0.002
29.129	3.0632	17	1	1	5	29.130	3.0631	0.001
29.409	3.0347	88	−1	3	1	29.405	3.0351	−0.004
29.671	3.0085	29	−1	3	2	29.684	3.0072	0.013
29.981	2.9781	19	1	2	5	29.940	2.9820	−0.041
30.132	2.9635	31	−1	3	0	30.127	2.9640	−0.005
30.563	2.9227	26	1	0	5	30.602	2.9190	0.039
30.686	2.9112	39	0	1	6	30.707	2.9093	0.021
31.013	2.8813	11	0	−2	4	30.996	2.8828	−0.017
31.186	2.8657	26	0	2	6	31.168	2.8673	−0.018
31.308	2.8548	32	0	4	1	31.288	2.8566	−0.020
31.887	2.8043	30	−1	1	5	31.898	2.8034	0.011
32.629	2.7422	21	0	4	0	32.659	2.7397	0.030
32.755	2.7319	28	0	4	4	32.791	2.7290	0.036
32.923	2.7183	9	−1	2	5	32.946	2.7165	0.023
33.676	2.6593	27	1	1	6	33.662	2.6603	−0.014
33.920	2.6407	24	2	1	1	33.940	2.6392	0.020
34.389	2.6057	64	2	1	2	34.388	2.6058	−0.001
34.533	2.5952	45	2	0	2	34.536	2.5950	0.003
34.899	2.5688	8	1	4	1	34.864	2.5713	−0.035
35.050	2.5581	9	0	4	5	35.045	2.5584	−0.005
35.371	2.5356	23	2	−1	1	35.368	2.5358	−0.003
35.692	2.5135	10	2	1	3	35.691	2.5136	−0.001
35.977	2.4943	15	−1	−1	5	35.971	2.4947	−0.006
36.057	2.4889	15	0	−1	6	36.024	2.4912	−0.033
36.232	2.4773	13	−1	4	2	36.227	2.4777	−0.005
36.400	2.4663	11	−1	4	1	36.406	2.4659	0.006
36.547	2.4567	15	−1	1	6	36.538	2.4573	−0.009
36.907	2.4335	14	−1	4	3	36.882	2.4351	−0.025
37.032	2.4256	9	2	2	3	37.049	2.4245	0.017
37.425	2.4010	13	1	−3	3	37.420	2.4014	−0.005
37.727	2.3825	12	−2	−1	2	37.733	2.3822	0.006
37.796	2.3783	17	2	1	4	37.771	2.3798	−0.025
37.970	2.3678	22	0	3	7	37.980	2.3672	0.010
38.383	2.3433	14	1	2	7	38.372	2.3439	−0.011
38.653	2.3275	32	2	−1	3	38.648	2.3278	−0.005
38.916	2.3124	10	0	5	2	38.908	2.3129	−0.008
39.094	2.3023	5	1	−2	5	39.117	2.3010	0.023
39.747	2.2660	11	2	3	2	39.749	2.2658	0.002
40.041	2.2500	9	1	3	7	40.025	2.2509	−0.016
40.136	2.2449	11	2	3	3	40.155	2.2438	0.019
40.419	2.2298	5	1	0	7	40.432	2.2291	0.013
40.529	2.2240	6	2	1	5	40.528	2.2241	−0.001
40.999	2.1996	15	2	2	5	41.015	2.1988	0.016
41.276	2.1855	9	0	2	8	41.284	2.1851	0.008
41.497	2.1744	11	0	4	7	41.512	2.1736	0.015
41.645	2.1670	12	1	−4	2	41.639	2.1672	−0.006
41.873	2.1557	4	−1	−3	4	41.886	2.1550	0.013
42.354	2.1323	7	−2	3	1	42.349	2.1326	−0.005
42.567	2.1221	16	0	3	8	42.604	2.1204	0.037
43.092	2.0975	15	−2	−3	1	43.066	2.0987	−0.026
43.328	2.0866	12	0	−5	1	43.333	2.0864	0.005
43.571	2.0755	7	0	5	6	43.560	2.0761	−0.011
43.733	2.0682	9	−1	5	3	43.757	2.0671	0.024
43.899	2.0608	11	1	−1	7	43.936	2.0591	0.037
44.067	2.0533	13	−1	5	1	44.050	2.0541	−0.017
44.29	2.0435	1	1	3	8	44.295	2.0433	0.005
44.711	2.0252	13	2	4	3	44.707	2.0254	−0.004
44.863	2.0187	9	−1	−4	3	44.831	2.0201	−0.032
45.299	2.0003	16	1	−3	5	45.269	2.0015	−0.030
45.495	1.9921	7	0	4	8	45.502	1.9919	0.007

Continued

https://doi.org/10.1017/S0885715617001129 Published online by Cambridge University Press

TABLE I. Continued

$2\theta_{obs}$ (°)	d_{obs} (Å)	$(I/I_0)_{obs}$	h	K	L	$2\theta_{calc}$ (°)	d_{calc} (Å)	$\Delta 2\theta$ (°)
46.189	1.9638	9	−1	−1	7	46.165	1.9648	−0.024
46.314	1.9588	8	−1	−3	5	46.323	1.9584	0.009
46.659	1.9451	9	0	2	9	46.657	1.9452	−0.002
47.053	1.9297	10	0	6	3	47.014	1.9313	−0.039
47.260	1.9218	14	0	−3	6	47.257	1.9219	−0.003
47.724	1.9042	9	−1	3	8	47.736	1.9037	0.012
47.951	1.8957	4	1	5	7	47.932	1.8964	−0.019
48.186	1.8870	6	1	2	9	48.178	1.8873	−0.008
48.277	1.8836	8	0	6	1	48.284	1.8834	0.007
48.454	1.8772	11	−2	1	6	48.445	1.8775	−0.009
48.750	1.8665	5	1	−2	7	48.754	1.8663	0.004
48.941	1.8596	3	1	1	9	48.945	1.8595	0.004
49.283	1.8475	6	1	6	4	49.284	1.8475	0.001
49.490	1.8403	12	0	0	9	49.506	1.8397	0.016
49.737	1.8317	7	2	−4	1	49.762	1.8309	0.025

C=N appears at 1610 cm^{-1} and one at 1644 cm^{-1} corresponds to C=O. The FT-IR spectrum (Figure 2) shows the bands characteristic of the functional groups in the material showing the chemical nature of the compound. Stretching O–H is overlapped by the bands of stretching N–H observed at 3351 cm^{-1} and the amide at 3161 cm^{-1} absorption bands widened by possibly Csp^2-H and Csp^3-H are observed at 3050 cm^{-1} and 2951 cm^{-1}, respectively. The characteristic band of the amide carbonyl (band I) is observed at 1557 cm^{-1} while the band II amide is observed at 1508 cm^{-1}. Other important bands are 1596 cm^{-1} to stretching C=C and 1333 cm^{-1} corresponding to the C–N vibration. In general, the spectrum shows absorption bands widened by possibly numerous hydrogen bonds in the structure.

Mirabegron melts at 142.96 °C, according to the first endotherm in DSC analysis (Figure 3). The TGA curve (Figure 3) shows that the material is stable up to 200 °C, experiencing weight loss 70.08% at ~206–426 °C. This corresponds to the total decomposition of mirabegron.

The indexing of pattern recorded (Figure 4) for the material was carried out with DICVOL14 (Boultif and Loüer, 2014). The analysis with NSB*AIDS83 (Mighell *et al.*, 1981), resulted in a triclinic unit cell P1 with parameters: $\boldsymbol{a} = 5.351(2)$ Å, $\boldsymbol{b} = 11.612(2)$ Å, $\boldsymbol{c} = 17.591(2)$ Å, $\alpha = 70.79(1)$, $\beta = 84.42(2)$, $\gamma = 86.29(2)$, $V = 1026.6(3)$ $Å^3$, and figures of merit associated are $M20 = 30.6$ and $F30 = 67.7$ (0.0085, 52) (de Wolf, 1968; Smith and Snyder, 1979). Table I contains the corresponding powder diffraction data. This pattern, in PD3 format, will be submitted for inclusion in the Powder Diffraction File. The space group is P1 with $Z = 2$, of the commercial material is chiral. The fitting of the whole pattern with the Le Bail algorithm in FULLPROF program (Rodriguez-Carvajal, 1990), using the above-mentioned unit cell parameters, accounts for all the diffraction maxima recorded. $Z = 2$ was estimated by density obtained by the flotation method ($d = 1.22(1)$ g cm^{-3}), and the calculated density, using this Z-value and the volume obtained from the indexing process, was 1.21 g cm^{-3}, similar to measured density.

SUPPLEMENTARY MATERIAL

The supplementary material for this article can be found at https://doi.org/10.1017/S0885715617001129.

ACKNOWLEDGEMENTS

The authors acknowledge the support of Vicerrectoría de Investigación y Extensión, Universidad Industrial de Santander (UIS) and Parque Tecnológico Guatiguará, UIS, Piedecuesta, Santander, Colombia, Laboratorio de Investigación en Polímeros for recording TGA-DSC data, Laboratorio de Espectroscopia for FT-IR and RAMAN spectra register and Laboratorio de Difracción de Rayos-X, for recording X-ray diffraction data.

Boultif, A. and Loüer, D. (**2014**). "Some further considerations in powder diffraction pattern indexing with the dichotomy method". Powd. Diffr. **29**(S2), S7–S12.

de Wolff, P. M. (**1968**). "A simplified criterion for the reliability of a powder pattern indexing," J. Appl. Crystallogr. **1**, 108–113.

Dong, C. (**1999**). "Powderx: windows-95-based program for poder X-ray diffraction data processing", J. Appl. Crystallogr. **32**, 838.

Groom, C. R., Bruno, I. J., Lightfoot, M. P., and Ward, S. C. (**2016**). "The cambridge structural database," Acta Crystallogr. Sect. B: Struct. Sci., Cryst. Eng. Mater. **72**, 171–179.

Mighell, A. D., Hubbard, C. R., and Stalick, J. K. (**1981**). *NBS* AIDS80: A Fortran Program for Crystalographic Data Evaluation*. (National Bureau Standards, USA), Technical Note 1141. (NBS*AIDS83is a newer versión of NBS*AIDS80).

Nitti, V., Khullar, V., van Kerrebroeck, P., Herschorn, S., Cambronero, J., Angulo, J., Blauwet, M., Dorrepaal, C., Siddiqui, E. and Martin, N. (**2013**). "Mirabegron for the treatment of overactive bladder: a prespecified pooled efficacy analysis and pooled safety analysis of three randomised, double-blind, placebo-controlled, phase III studies". Int. J. Clin. Pract. **67**(7), 619–632.

Rachinger, W. A. (**1948**). "A correction for the α_1 α_2 doublet in the measurement of widths of X-ray diffraction lines", J. Sci. Instrum. **25**, 254.

Rodriguez-Carvajal, J. (**1990**). "FULLPROF: a program for Rietveld refinement and pattern matching analysis," in Abstracts of the Satellite Meeting on Powder Diffraction of the XV Congress of the IUCr, Toulouse, France, p. 127.

Savitzky, A. and Golay, M. J. (**1964**). "Smoothing and differentiation of data by simplified least squares procedures". Anal. Chem. **36**, 1627–1639.

Smith, G. S. and Snyder, R. L. (**1979**). "FN: a criterion for rating powder diffraction patterns and evaluating the reliability of powder-pattern indexing". J. Appl. Crystallogr. **12**, 60–65.

Sonneveld, E. J. and Visser, J. W. (**1975**). "Automatic collection of powder diffraction data from photographs". J. Appl. Crystallogr. **8**, 1–7.